World Cancer Research Journal

WCRJ 2026; 13: e2997
DOI: 10.32113/wcrj_20262_2997

CXCL10 IN OVARIAN CANCER: BIOINFORMATICS ANALYSIS OF ITS PROGNOSTIC VALUE AND IMMUNE REGULATORY ROLE

L. DENG[1], W.-H. LIN[1], F.-M. JIAN[1], D.-S. FAN[1], J.-M. LAN[2], D.-X. LIAO[3], P.-Y. LUO[1]

• • •

[1]Department of Pharmacy, Longyan First Affiliated Hospital of Fujian Medical University, Longyan, 364000, China
[2]The School of Pharmacy, Fujian Medical University, Fuzhou, 350000, China
[3]Department of Oncology, Longyan First Affiliated Hospital of Fujian Medical University, Longyan, 364000, China

Corresponding Author
Peiyuan Luo, MD; email: 13806988586@163.com

ABSTRACT – *Objective:* This study aimed to explore the potential prognostic value and immunoregulatory roles of C-X-C motif chemokine ligand 10 (CXCL10) in ovarian cancer through bioinformatics analysis to identify potential biomarkers for personalized immunotherapy strategies.

Materials and Methods: We integrated Genotype-Tissue Expression (GTEx) normal ovarian tissues (n=88) and The Cancer Genome Atlas (TCGA) ovarian cancer samples (n=427) to screen differentially expressed genes using DESeq2 (version 1.42.0) and limma (version 3.40.2) packages. Protein-protein interaction networks (PPI) were constructed *via* Search Tool for the Retrieval of Interacting Genes (STRING) and Cytoscape (version 3.10.1). Survival analysis was performed with Kaplan-Meier method and pathway enrichment was analyzed through Gene Ontology (GO), Kyoto Encyclopedia of Genes and Genomes (KEGG), and Gene Set Enrichment Analysis (GSEA). Immune infiltration was assessed using Cell-type Identification by Estimating Relative Subsets of RNA Transcripts (CIBERSORT) algorithm. Validation was conducted using GEO datasets (GSE10971, GSE14407, GSE18520) and experimental verification through quantitative PCR (qPCR), Western blot, and Cell Counting Kit-8 (CCK-8) assays in ovarian cancer cell lines.

Results: CXCL10 expression was significantly upregulated in ovarian cancer tissues compared to normal tissues ($p<0.001$) and showed correlation with T-cell and macrophage infiltration ($p<0.001$). Patients with low CXCL10 expression had poor prognosis (HR < 1), while co-expression with immune checkpoint molecules programmed cell death protein 1 (PDCD1), T cell immunoreceptor with Ig and ITIM domains (TIGIT), and forkhead box P3 (FOXP3) was associated with longer survival. Functional enrichment analysis revealed that CXCL10 was significantly enriched in immune-related pathways including lymphocyte-mediated immune response and antigen presentation. Correlation analysis demonstrated strong associations between CXCL10 and immune checkpoint genes including PDCD1 and CTLA-4 ($p<0.05$). The time-dependent ROC analysis showed limited individual prognostic capability with AUC values of 0.446 for CXCL10, 0.478 for PDCD1, 0.435 for TIGIT, and 0.455 for FOXP3. Experimental validation confirmed that CXCL10 overexpression inhibited A2780 and SKOV3 cell proliferation ($p<0.01$) and enhanced the efficacy of anti-PD-1 antibodies.

Conclusions: Our findings suggest that CXCL10 may serve as a potential prognostic biomarker and immunotherapeutic target for ovarian cancer. The results indicate possible clinical applications in patient stratification and combination immunotherapy strategies, though further mechanistic studies and clinical validation are warranted.

KEYWORDS: CXCL10, Ovarian cancer, Prognostic biomarker, Immune regulation, Bioinformatics analysis.

INTRODUCTION

Ovarian cancer is a common gynecological malignancy with significant heterogeneity and a complex tumor microenvironment[1]. Although surgery and chemotherapy have advanced, most patients still experience recurrence and treatment resistance, leading to poor prognosis[1,2]. Recent advances in understanding the immune microenvironment have revealed the complexity of tertiary lymphoid structures and immune cell interactions in ovarian cancer, though immune checkpoint inhibitors demonstrate limited efficacy compared to other cancer types[3-5].

Programmed cell death protein 1 (PD-1 or PDCD1)/programmed death-ligand 1(PD-L1 or CD274) inhibitors are important immune checkpoint inhibitors (ICIs) that restore T-cell function by blocking the PD-1/PD-L1 interaction[6]. Cytotoxic T-lymphocyte-associated protein 4 (CTLA4) inhibitors promote T-cell activation by blocking CTLA-4 binding to its ligands[7]. A recent study has identified novel immune regulatory mechanisms involving TIGIT-NECTIN2 interactions and the CD47/TSP-1 axis in ovarian cancer[5]. Furthermore, novel immune checkpoint inhibitors, such as lymphocyte-activation gene 3 (LAG-3) and T-cell immunoglobulin and mucin-domain containing-3 (TIM-3), are under intensive investigation[8,9]. Nonetheless, the overall response rate to ICIs for ovarian cancer remains suboptimal, highlighting the urgent need to explore combination therapies involving chemotherapy, targeted therapies, and other immunotherapeutic strategies[6-8,10].

C-X-C motif chemokine ligand 10 (CXCL10), classified within the CXC chemokine family, is primarily secreted by immune cells, particularly dendritic cells and macrophages[11]. Many factors influence CXCL10 regulation, including various inflammatory cytokines, important growth factors, and key signaling molecules within the tumor microenvironment[12]. CXCL10 exerts its effects through several signaling pathways. Activation of the phosphatidylinositol 3-kinase/protein kinase B/mechanistic target of rapamycin (PI3K/AKT/mTOR) pathway influences cellular growth, survival, and metabolism[13]. In ovarian cancer cells, this pathway's activation is closely associated with tumor progression and the development of drug resistance. Furthermore, CXCL10 promotes cellular migration and invasion through the mitogen-activated protein kinase (MAPK) pathway by regulating cytoskeletal dynamics and extracellular matrix degradation[14]. Moreover, CXCL10 modulates immune response pathways and inflammatory processes *via* the Janus kinase/signal transducer and activator of transcription (JAK/STAT) signaling pathway, thereby impacting cytokine production and immune cell function[15]. It also exhibits anti-angiogenic properties[16]. During inflammation, CXCL10 promotes immune cell chemotaxis and activation, thereby modulating the inflammatory microenvironment[12].

Despite extensive research on the ovarian cancer immune microenvironment, systematic studies specifically focusing on CXCL10's role in ovarian cancer remain limited. Both tumor and stromal cells can produce CXCL10, and preliminary evidence suggests its expression may be elevated in ovarian cancer tissues and correlate with cancer progression and patient prognosis[17]. Developing therapeutic strategies targeting CXCL10 may enhance the efficacy of ICIs and may hold significant clinical potential in treating ovarian cancer. This study aims to elucidate the role of CXCL10 in ovarian cancer progression and investigate its potential to synergize with ICIs to improve treatment outcomes in ovarian cancer patients.

MATERIALS AND METHODS

Dataset Download and Processing

This study aimed to obtain RNA sequencing from both normal ovarian tissues and ovarian neoplasm specimens. We initially downloaded RNA-Seq data of normal ovarian tissues from the Genotype-Tissue Expression (GTEx) database (https://gtexportal.org/home/datasets[18]). Subsequently, we obtained RNA-Seq data of ovarian cancer specimens from The Cancer Genome Atlas (TCGA) portal[19] (https://portal.gdc.cancer.gov/). Quality control measures included filtering samples with low RNA integrity scores (<6.0) and removing samples with insufficient clinical annotation. After quality control and data preprocessing, we processed the data using R and Bioconductor packages. The analysis pipeline involved loading required R packages, such as DESeq2 [version 1.42.0] and tximport [version 1.14.0][20]. Transcript-level counts were summarized to Transcripts Per Million (TPM) using tximport, following established protocols[21]. After processing, we used the dplyr [version 0.8.1] package to merge the TPM-normalized data from GTEx and TCGA into a combined expression matrix. To ensure comparability, we then standardized the integrated data and subjected to downstream bioinformatics analyses at both sample and gene expression levels.

Differential expression analysis

Gene expression data and clinical information from the Cancer Genome Atlas Ovarian Cancer (TCGA-OV) cohort were integrated with normal ovarian tissue data from the GTEx database. All data were standardized to TPM format for consistency. The limma [version 3.40.2] package in R was utilized to analyze gene expression differences, producing a set of differentially expressed genes (DEGs) set A. Visualization of these DEGs was achieved through heatmaps and volcano plots. We established screening criteria by selecting genes with |logFC| > 0.58 and *p*-value < 0.05. This allowed us to identify statistically significant differentially expressed genes[22]. Subsequently, we retrieved a chemokine-related gene set from the Gene Set Enrichment Analysis (GSEA) database. Then, the VennDiagram [version 1.6.20] package in R was used to identify the intersection between the GTEx-TCGA_OV DEG set and the chemokine gene set B[23]. "GTEx-TCGA_OV DEG" refers to a subset of DEGs identified by comparing ovarian tumor tissues from TCGA-OV with healthy ovarian tissues from the GTEx project.
To validate these findings, differential expression analysis was conducted using three independent GEO datasets (GSE10971[24], GSE14407[25], and GSE18520[26]) comparing ovarian cancer and normal samples. Principal Component Analysis (PCA) was performed to assess the overall data structure. Volcano plots and Venn diagrams were generated to visualize significant DEGs and their overlap across datasets. Heatmaps depicted the expression patterns of key DEGs, including chemokines such as CXCL10[27].

Protein-Protein Interaction Network (PPI) Analysis

This study utilized three main data sets: the Overall Survival (OS) prognostic gene set, the differential gene set from GTEx-TCGA_OV, and chemokines set. The top 100 differentially expressed prognostic gene set and the differentially expressed chemokine gene set were identified using the ggplot2 [version 3.4.4][28] and VennDiagram [version 1.6.20][29] packages. Subsequently, the protein-protein interaction network (PPI) was constructed using these combined gene sets via the STRING database[30]. The resulting network was imported into Cytoscape software (version 3.10.1), and key hub genes were identified.

Functional Enrichment Analysis

This study analyzed CXCL10 expression levels in ovarian cancer by dividing samples into high and low groups and screened for relevant differentially expressed genes. Gene expression data were sourced from the TCGA database and were grouped based on the median CXCL10 expression. The R package limma [version 3.40.2][22] was used for screening using criteria of |log2 fold change| > 1 and *p*-value < 0.05. Gene annotation was performed using the R package org.Hs.eg.db [3.3.0]. Gene Ontology (GO) and Kyoto Encyclopedia of Genes and Genomes (KEGG) enrichment analyses were conducted using the clusterProfiler [version 3.14.0][31] package with $p < 0.05$ as the significance threshold. Gene Set Enrichment Analysis (GSEA) was performed using the fgsea [version 1.10.0][32] package to assess gene enrichment with a significance threshold of $p < 0.05$. All results were visualized using R software. Plots were generated with the ggplot2 package [version 3.4.4] and significance was indicated by Log10(p.adjust).

Correlation Analysis of CXCL10 with Immune Checkpoints and Immune Cells

Bioinformatics approaches were used to analyze CXCL10 expression levels in ovarian cancer tissues and to investigate their correlation with clinical features. Data from TCGA and GEO databases were used to generate a Venn diagram identifying significantly differentially expressed genes, especially chemokine genes linked to prognosis. The STRING database constructed the PPI analysis to identify key genes, whose correlation with T cell-associated immune checkpoints was then analyzed[30,33]. We used the ggplot2 [version 3.4.4] and ComplexHeatmap [2.13.1] packages to generate heatmaps that showed the expression trends of key immune genes. Additionally, the Cell-type Identification by Estimating Relative Subsets of RNA Transcripts (CIBERSORT)[34] algorithm was applied to assess the proportions of various immune cell types and analyze their relationship with CXCL10 expression regarding immune cell infiltration. The results were displayed through bubble plots. All statistical analyses were performed using R, applying the limma [version 3.40.2] package for differential expression analysis with a significance threshold set at $p < 0.05$.

This study also used bioinformatics methods to analyze the differential expression of CXCL10 and key immune checkpoint genes, such as PDCD1 and TIGIT. It also analyzed their effects on patient survival. Box plots were used to display gene expression levels across different groups, enabling straightforward comparison. TCGA-OV patients were stratified into high and low expression groups for each gene based on median expression levels. Kaplan-Meier survival analysis and log-rank tests were performed using the survival [version 3.3.1] package to assess prognostic significance[35,36]. Furthermore, the ggplot2 [version 3.4.4] package was used to visualize the correlation between CXCL10 and the 24 immune cell types. Subsequently, we focused on the examining the infiltration of key T cell subsets (including CD8+ T cells and Th1 cells) and activated dendritic cells (aDC) in relation to CXCL10. This analysis was visualized using scatter plots.

Assessment of Clinical Predictive Efficacy of CXCL10, PDCD1, TIGIT, and FOXP3

The prognostic value of CXCL10, PDCD1, TIGIT, and FOXP3 for overall survival was assessed. Initially, time-dependent receiver operating characteristic (ROC) curve analyses were performed at multiple time intervals to evaluate prognosis. Expression data of relevant genes were retrieved from the TCGA database, and the area under the curve (AUC) for each gene was calculated using the timeROC [version 0.4] package[37,38]. A prognostic nomogram[37,39,40] incorporating CXCL10 expression, PDCD1 expression, TIGIT expression, FOXP3 expression, and clinical parameters (stage, age, histological grade, venous invasion status) was developed using the TCGA-OV cohort. The nomogram was constructed and visualized using the survival [version 3.3.1] and rms [version 6.3.0] packages. Calibration curves were generated to assess the nomogram's predictive accuracy. Additionally, diagnostic ROC curve analyses were performed using the pROC [version 1.18.0] package to validate the predictive power of CXCL10 and other immune checkpoint genes (PDCD1, TIGIT, FOXP3, interleukin 17A (IL17A), and CD274) in survival prediction[37,41,42].

Expression and Functional Study of CXCL10 in Ovarian Cancer Cells

Total RNA was isolated from ovarian cancer cell lines (OVCAR3, SKOV3, A2780, and ES2; ProCell) using the RNA extraction kit (Vazyme, RC112-01) for cell samples. Purified RNA was reverse-transcribed to cDNA with the cDNA synthesis kit (TransGen, AT341-02). Relative CXCL10 mRNA expression levels were quantified by real-time quantitative PCR (qPCR) using SYBR Green Master Mix (Vazyme, Q321). Primers for CXCL10 (F: 5'-CCTGCAAGCCAATTTTGTCC-3', R: 5'-AGACCTTTCCTTGCTAACTGC-3') and the reference gene β-actin (ACTB) (F: 5'-GAAAATCTGGCACCACACCTTC-3', R: 5'-ATGATCTGGGTCATCTTCTCGC-3') were used. Data were analyzed using the $2^{-\Delta\Delta Ct}$ method. Lentiviral vectors for CXCL10 overexpression (OE) and knockout (KO; using Cas9-sgRNA system) were constructed. Lentiviruses were produced by co-transfecting 293T cells (ProCell, CL-0005) with the transfer vector and packaging plasmids (psPAX2 and pMD2.G). SKOV3 (ProCell, CL-0215) and A2780 (ProCell, CL-0013) cells were transduced with lentiviruses in the presence of polybrene (8 μg/mL). Fluorescence signal in transduced cells was examined under a fluorescence microscope to confirm transduction efficiency. Overexpression and knockout efficiency were confirmed by Western blot. Finally, densitometric analysis was conducted using ImageJ software [version 1.52] to calculate relative protein expression, allowing comparison among control, overexpression, and knockout groups.

Assessment of Sensitivity to Immune Checkpoint Inhibitors and Changes in Cell Proliferation and Immune Cell Subpopulations

To predict the association between CXCL10 expression and response to immune checkpoint blockade, data from The Cancer Immunome Atlas (TCIA)[39,40] (https://tcia.at/) for Skin Cutaneous Melanoma (SKCM) and Ovarian Cancer (OV) were utilized. Patients were classified into high and low expression groups based on CXCL10 levels. The Immunophenoscore (IPS) for each patient, representing predicted response to CTLA-4 and PD-1 blockade, was extracted. IPS scores were compared between high and low CXCL10 groups within each cancer type using the Mann-Whitney U test. The effect of CXCL10 expression on tumor cell proliferation and response to anti-PD-1 therapy was assessed *in vitro*. A2780 and SKOV3 cells with stable CXCL10 overexpression (OE), knockout (KO), or vector control (Ctrl) were co-cultured with allogeneic PBMCs at a tumor cell:PBMC ratio of 1:5 in RPMI-1640 medium supplemented with 10%

FBS. Co-cultures were treated with anti-PD-1 monoclonal antibody (10 µg/mL; Pembrolizumab biosimilar). Docetaxel (5 µg/mL) was used as a positive control for cytotoxicity. After 72 hours of co-culture, cell proliferation was measured using the CCK-8 assay. The experiment was performed in triplicate and repeated three times independently.

Statistical Analysis

This study used various statistical methods to evaluate the significance and correlations in the experimental data. Specifically, comparative analyses among groups used either one-way ANOVA or *t*-tests, depending on whether the data distribution was normal.

RESULTS

Differential Expression Analysis

Figure 1 shows the study workflow. We analyzed gene expression in normal ovarian samples from the GTEx database and ovarian cancer (OV) samples from the TCGA repository. This analysis identified 2,711 significantly upregulated genes and 4,422 downregulated genes (Figure 2A). The top ten upregulated genes included SLC34A2, KRT7, S100A1, PLOD1, KRT5, CLDN3, SLPI, CD24, MSLN, and CLDN4, while the top ten downregulated genes included CCDC53, PUS1, MTAP, AKR1C1, SLC7A10, SERPINA1, CCL18, ZNF36L1, GIMAP4, and GIMAP5. A heatmap (Figure 2B) illustrated the top 25 differentially expressed genes in normal and ovarian cancer samples. Analysis using a Venn diagram (Figure 2C) revealed 20 upregulated and 4 downregulated chemokine genes. These findings provided a basis for subsequent chemokine investigations. Differential expression analysis of chemokines (Figure 2D) revealed significant upregulation of CXCL10 and C-X-C motif ligand 11 (CXCL11) ($p < 0.01$). A boxplot (Figure 2E) further supported

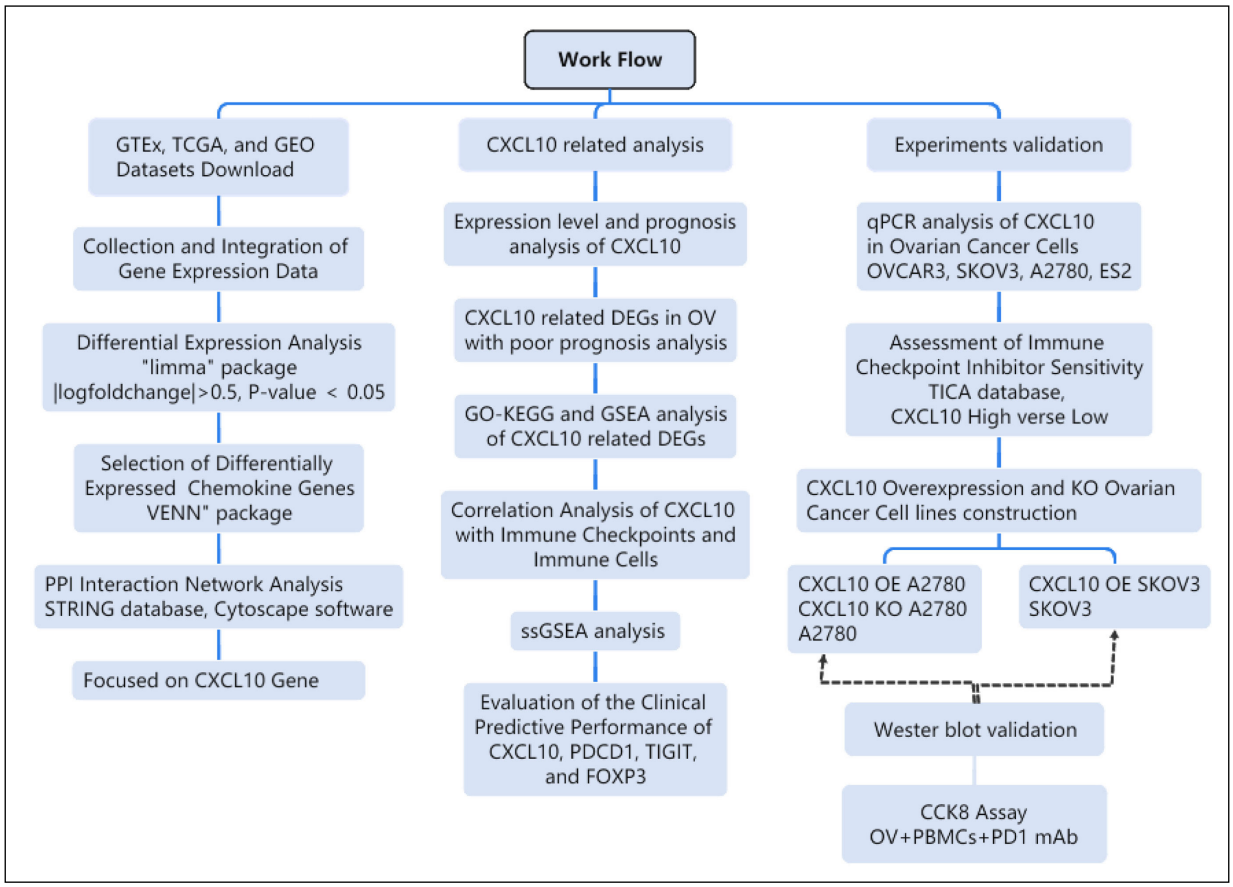

Figure 1. The workflow of the study.

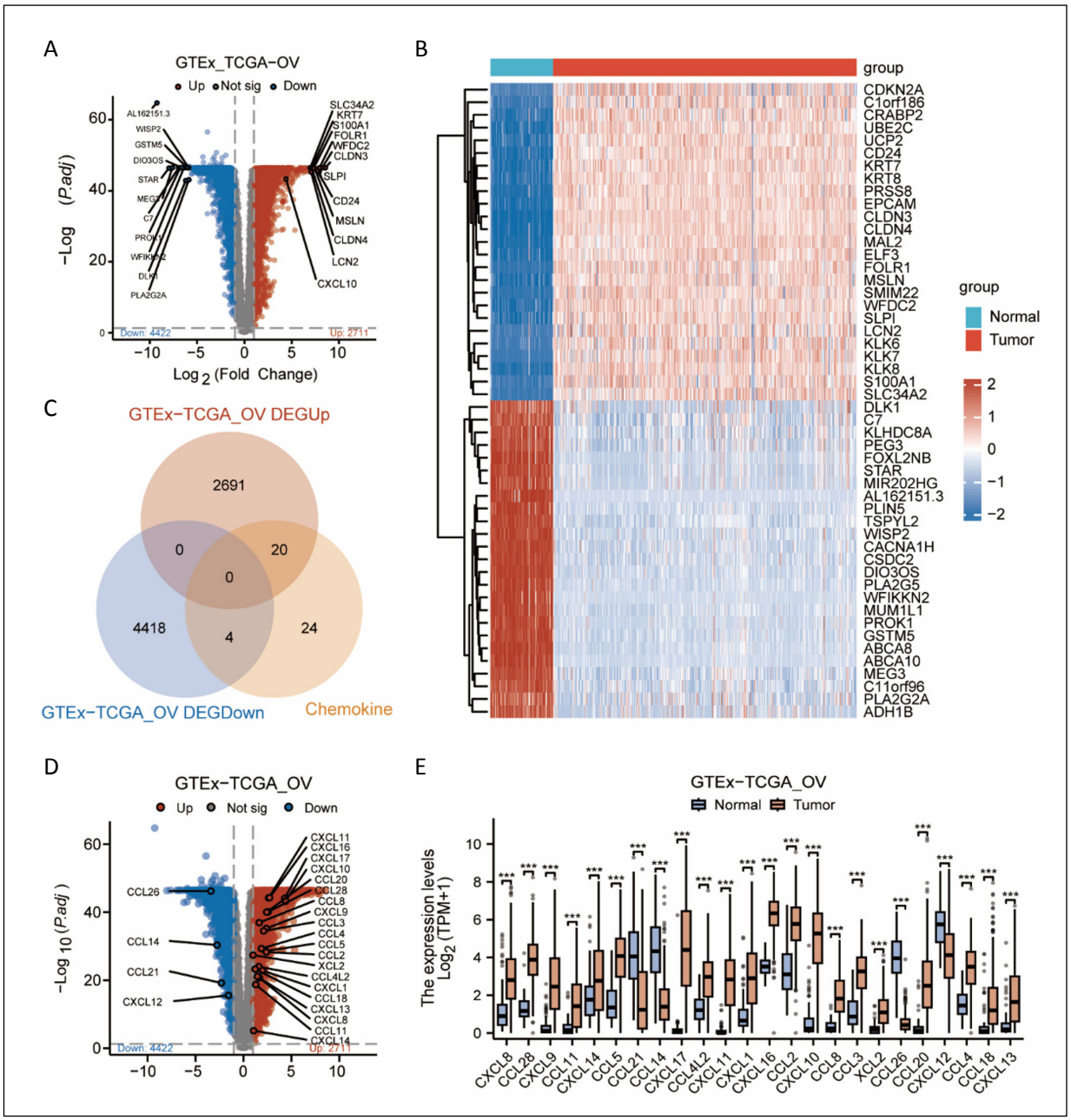

Figure 2. Differential gene expression analysis of GTEx-TCGA ovarian cancer (GTEx-TCGA_OV). *A*, Volcano plot shows differentially expressed genes. *B*, Heatmap displays gene expression differences. *C*, Venn diagram illustrates upregulated and downregulated genes, as well as chemokines. *D*, Volcano plot showing differentially expressed chemokine genes. *E*, Box plot compares chemokine expression levels. Statistical significance is indicated as follows: *** $p < 0.001$; ** $p < 0.01$; * $p < 0.05$.

these conclusions, demonstrating that the expression levels of these chemokines were substantially increased in ovarian cancer samples compared to normal specimens, suggesting their potential roles in the tumor microenvironment. Our study identified upregulation of specific genes and chemokines, especially CXCL10 and CXCL11, suggesting their key roles in ovarian cancer development. Further research is needed to explore their utility as therapeutic targets or biomarkers.

We performed a systematic analysis of microarray data from GSE10971, GSE14407, and GSE18520. The GEO chip data indicated the elevated expression of key chemokines, especially CXCL10, in ovarian cancer samples, providing vital insights for further mechanistic investigations (Supplementary Figure 1). Additionally, we performed extensive validation using the GSE10971 dataset, focusing specifically on chemokine-related differential genes and gene sets (Supplementary Figure 2). The outcomes of our study suggested that CXCL10 might play a pivotal role in the initiation and progression of ovarian cancer.

Protein-Protein Interaction Network Analysis

Venn diagram analysis demonstrated the overlap among three gene sets: those associated with ovarian cancer prognosis, differentially expressed genes from GTEx and TCGA_OV, and chemokine genes (Figure 3A). From this analysis, we identified eight differentially expressed chemokines were identified. These chemokines were prognostically significant and might play important roles in tumor progression. The PPI network analysis revealed strong interactions among the top 100 critical molecules using STRING database (confidence score > 0.4) and Cytoscape visualization (Figure 3B). Notably, several upregulated genes, including CXCL10 and serpin family B member 3 (SERPINB3) were involved (Figure 3B). The analysis showed a significant increase in CXCL10 expression in the tumor cohort ($p < 0.001$). Additionally, C-X-C motif chemokine ligand 9 (CXCL9) and CXCL11 also showed significant increases ($p < 0.01$) (Figure 3C). Moreover, the heatmap confirmed the substantial upregulation of CXCL10 and other key genes (Figure 3D). Collectively, these findings emphasized the importance of further research into the biological roles of these chemokines in ovarian cancer progression, their potential as diagnostic and therapeutic targets, and their variable expression across different cancer microenvironments.

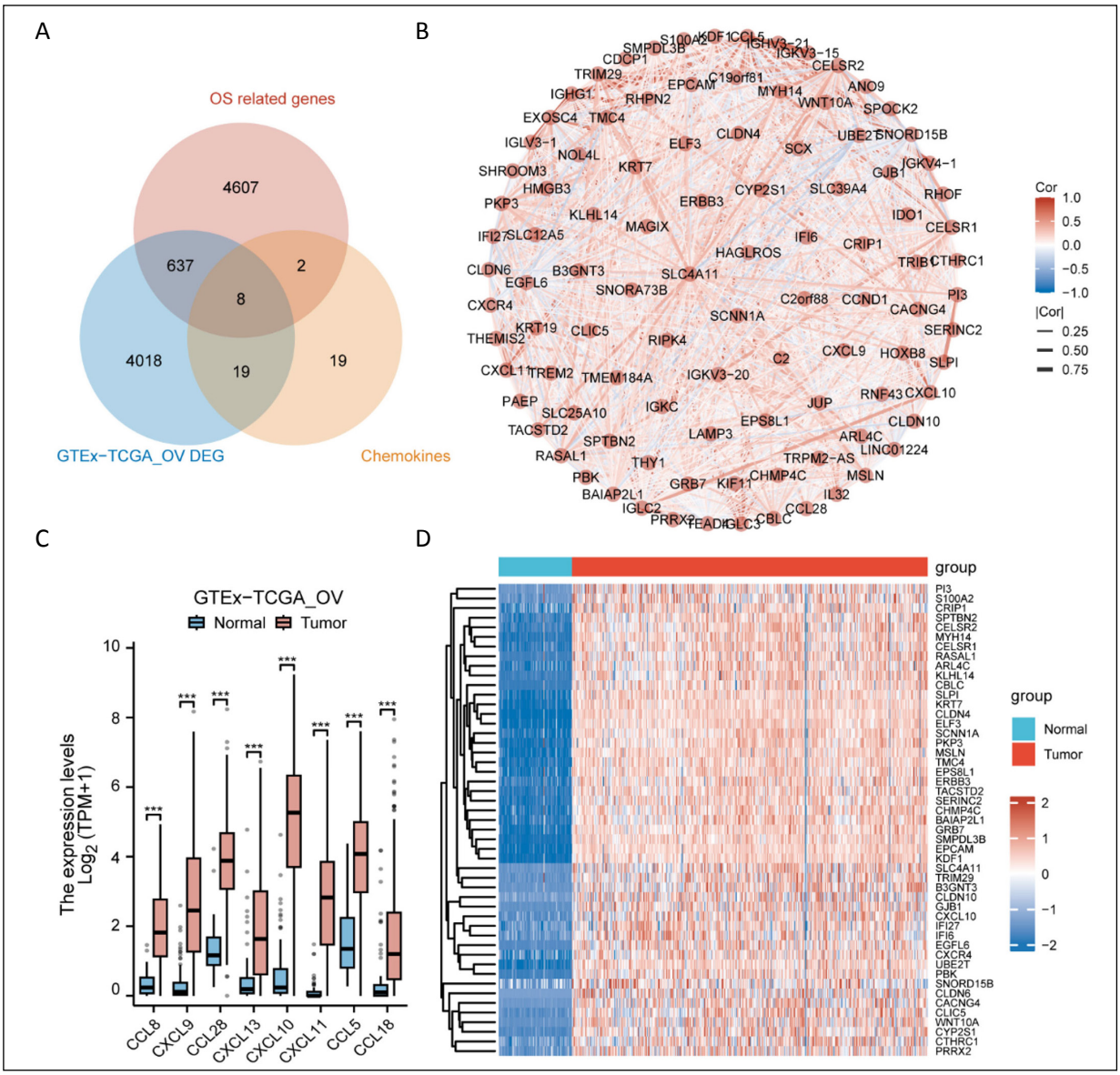

Figure 3. Analysis of prognostic molecules related to ovarian cancer, differentially expressed genes in GTEx-TCGA_OV, and chemokine gene expression. *A*, Venn diagram shows the overlap among ovarian cancer-related genes, differentially expressed genes from GTEx-TCGA_OV, and chemokine genes. *B*, The protein-protein interaction (PPI) network of the intersecting molecules highlights key interactions. *C*, Comparison of the expression levels of differentially expressed chemokine genes between normal and tumor samples is shown. *D*, Heatmap shows the expression patterns of upregulated genes. Statistical significance is indicated as follows: *** $p < 0.001$, ** $p < 0.01$, * $p < 0.05$.

Functional Enrichment Analysis (GO-KEGG and GSEA)

Figure 4 showed results from three analyses related to differential gene sets associated with CXCL10 expression in ovarian cancer: GO functional enrichment, KEGG pathway, and GSEA. The results indicated that CXCL10 was significantly enriched in key biological processes such as "lymphocyte-mediated immune response" and "antigen presentation," underscoring its critical role in immune responses (Figure 4A). Additionally, the analysis confirmed the significant role of CXCL10 in activating T cells and dendritic cells (Figure 4B). The enrichment scores (normalized enrichment score [NES] values) showed that the high CXCL10 expression group exhibited significant activation in key signaling pathways, including mitochondrial calcium mobilization. These findings highlighted the importance of calcium signaling in regulating immune cell functions (Figure 4C). Finally, the ranking plot from the GSEA analysis revealed that samples with high CXCL10 expression were significantly enriched in multiple major immune pathways, further corroborating its central role in promoting immune activity (Figure 4D). These functions sug-

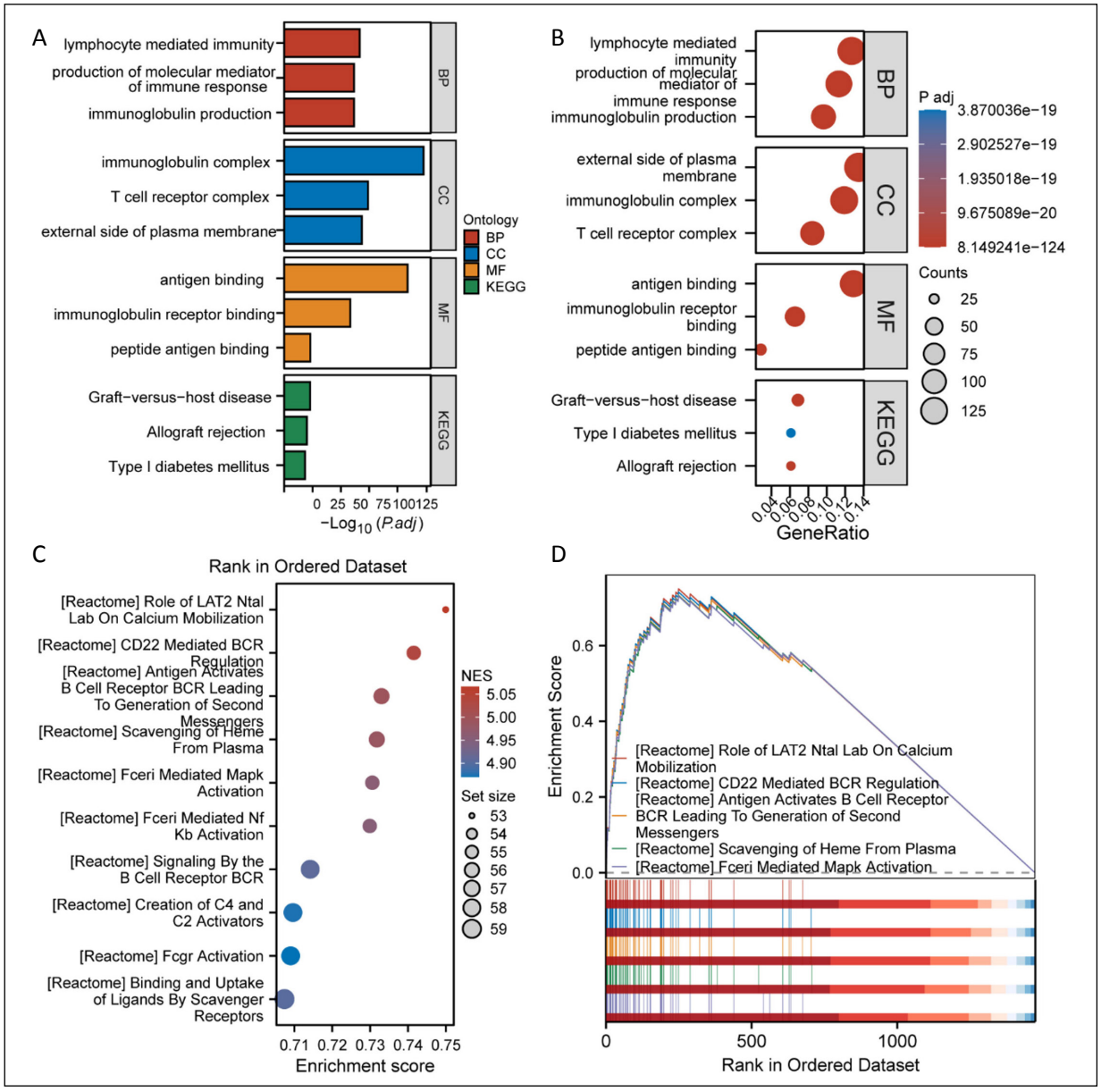

Figure 4. Gene Ontology (GO), Kyoto Encyclopedia of Genes and Genomes (KEGG), and Gene Set Enrichment Analysis (GSEA) in ovarian cancer samples based on high and low C-X-C motif chemokine ligand 10 (CXCL10) expression. *A*, The GO and KEGG analyses highlight key biological processes associated with CXCL10 and identify their enrichment levels. *B*, The statistical significance of various pathways in the high CXCL10 expression group is shown based on GO and KEGG analyses. *C*, Enrichment scores for pathways across the ordered dataset are presented, including normalized enrichment scores (NES) and rank positions. *D*, GSEA results illustrate differences in pathway enrichment scores across samples with high CXCL10 expression. Statistical significance is indicated as follows: *** $p < 0.001$; ** $p < 0.01$; * $p < 0.05$.

gested that CXCL10 had potential as both a biomarker and a therapeutic target in anti-tumor immunotherapy. Therefore, future studies should focus on elucidating the precise mechanisms by which CXCL10 interacted with other immune components, particularly its role in promoting immune cell infiltration within the tumor microenvironment. Understanding these complex dynamics could provide significant insights for developing novel immunotherapeutic strategies designed to enhance patient outcomes.

Correlation Analysis of CXCL10 with Immune Checkpoints and Immune Cells

This study identified 127 differentially expressed genes related to prognosis, including 7 chemokine genes. These genes were identified by integrating gene expression data from the GTEx-TCGA_OV dataset. We then analyzed differentially expressed genes related to overall survival (OS) in conjunction with the chemokine gene set (Figure 5A). A comprehensive analysis of the PPI network revealed that CXCL10 interacted with its related genes (Figure 5B), highlighting CXCL10's strong connection with numerous immune cell-related genes. The correlation heatmap analysis showed strong correlations between CXCL10 and immune checkpoint genes, including PDCD1 and CTLA-4 ($p < 0.05$) (Figure 5C). Furthermore, it highlighted a significant correlation between CXCL10 expression and the density of T cells and macrophages present (Figures 5D and 5E). The bubble plot showed the infiltration levels of various immune cell types in relation to CXCL10 expression. Bubble size and color indicated the strength and direction of these associations, highlighting particularly strong links with T cell subsets, such as regulatory T cells (Tregs), T helper 1 (Th1) cells, and cytotoxic T cells (Figure 5F).

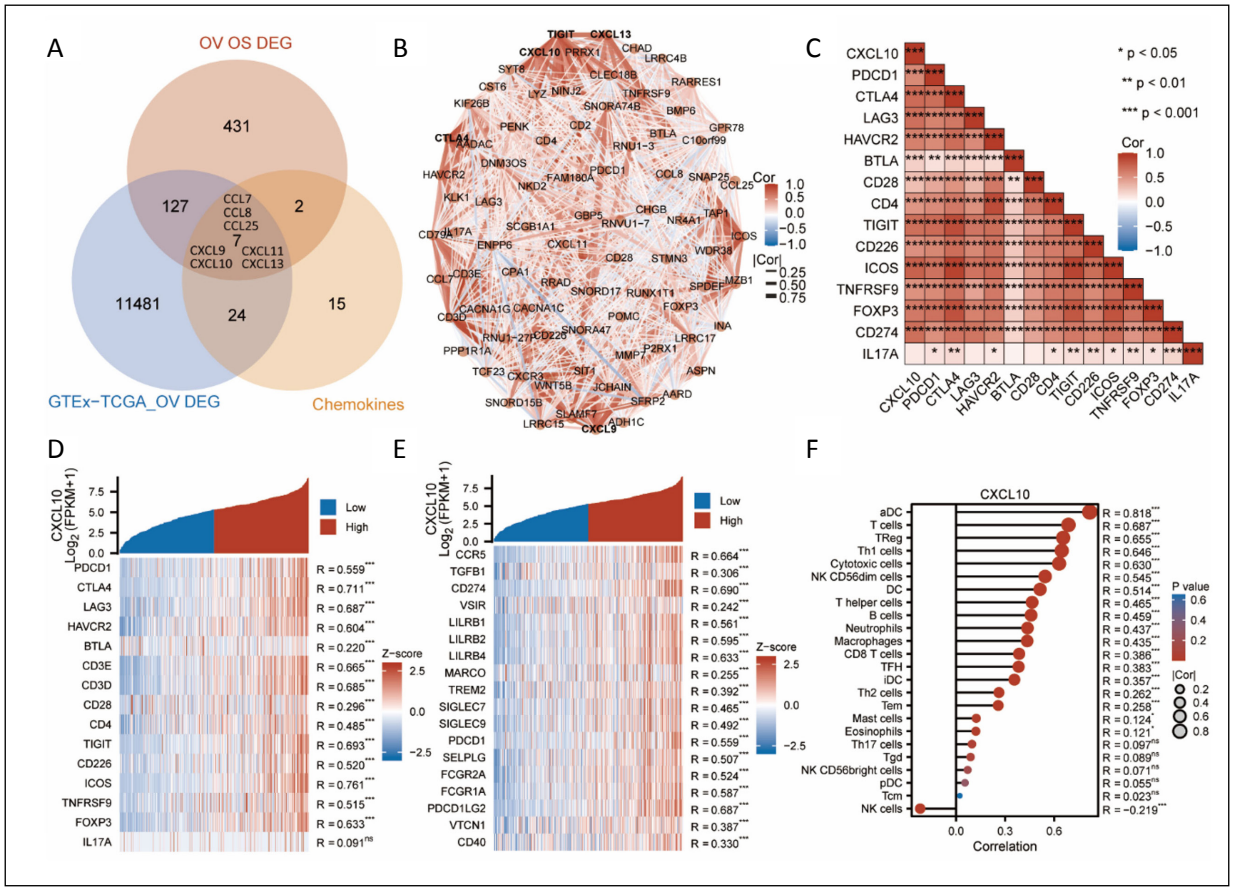

Figure 5. Examination of C-X-C motif chemokine ligand 10 (CXCL10) within neoplastic tissues and its association with immune cell infiltration. *A*, A Venn diagram showed the overlap of significantly differentially expressed genes from three datasets: ovarian cancer overall survival (OS)-related differentially expressed genes (DEGs) (OV OS DEG), GTEx-TCGA_OV DEGs, and chemokines. *B*, A protein-protein interaction (PPI) network illustrates the interactions between CXCL10 and its related genes. *C*, A heatmap shows the correlations between CXCL10 and immune checkpoint genes, including correlation coefficients and significance levels. *D-E*, Heatmaps display the expression profiles of CXCL10 together with immune checkpoint genes expressed in T cells and macrophages, highlighting their differential expression patterns. *F*, A bubble plot illustrates the correlation between CXCL10 and immune cell infiltration levels, with bubble color and size indicating infiltration degree. Statistical significance is indicated as follows: *** $p < 0.001$; ** $p < 0.01$; * $p < 0.05$.

These results suggested that high CXCL10 levels might enhance the immune response by recruiting T cells. In summary, these findings demonstrated that CXCL10 was highly expressed in ovarian tumor tissues and closely linked to diverse immune checkpoints and immune cell infiltration, suggesting its pivotal role in the immune microenvironment and potential as a clinical therapeutic target.

Bioinformatics Analysis of CXCL10 and Immune Checkpoint Gene Expression Differences

This investigation examined the relationship between CXCL10 and key immune checkpoint genes: PDCD1, TIGIT, FOXP3, and CD274. Additionally, it explored their implications for ovarian cancer prognosis using bioinformatics analysis. Scatterplot analyses revealed strong positive correlations between CXCL10 and PDCD1, TIGIT, and FOXP3, but no significant correlation between CXCL10 and cytokine IL17A. Furthermore, survival curve analysis (Supplementary Figure 3) showed that patients with elevated expression levels of CXCL10, PDCD1, TIGIT, and FOXP3 had significantly prolonged survival compared to those with lower expression, with hazard ratios (HRs) all below 1. This underscored their potential applicability as favorable prognostic markers. Overall, these findings highlighted the notable contribution of CXCL10 and T cell-related immune checkpoints in the tumor immune microenvironment, suggesting CXCL10 as a promising prognostic biomarker.

Correlation Analysis of CXCL10 and Immune Cell Infiltration

This research investigated the association between CXCL10 and the infiltration of 24 immune cell types. We used Spearman correlation to assess the relationship between CXCL10 and various immune cell populations (Supplementary Figure 4A). Scatter plots (Supplementary Figures 4B-S4J) revealed significant positive correlations between CXCL10 and several T cell subtypes, including cytotoxic T cells, Th1 cells, Treg cells, and T helper 2 (Th2) cells. Future studies should clarify the function and pathways of CXCL10 in ovarian carcinoma and other tumors in order to better evaluate its potential as a therapeutic target. Despite challenges like data complexity and variability in immune cell infiltration, future studies should combine clinical specimens with animal models for more comprehensive analysis.

Assessment of Clinical Predictive Efficacy of CXCL10, PDCD1, TIGIT, and FOXP3

In this study, we used advanced bioinformatics methods to evaluate four biomarkers: CXCL10, PDCD1, TIGIT, and FOXP3. We further assessed their ability to predict survival outcomes in ovarian cancer patients. The analysis revealed time-dependent ROC AUC values of 0.446 for CXCL10, 0.478 for PDCD1, 0.435 for TIGIT, and 0.455 for FOXP3, indicating limited prognostic capability of these biomarkers when considered independently (Figure 6A). Nonetheless, the nomogram-derived calibration curves exhibited good concordance between the predicted survival probabilities and the empirically observed survival rates at 1, 3, and 5 years ($p < 0.01$) (Figure 6B). The results showed that biomarker scores significantly correlated with clinical features, including pathological grading and staging, effectively predicting patient survival. By integrating clinical characteristics with biomarker scores, the nomogram offered an innovative and comprehensive strategy for individualized survival prediction (Figure 6C). ROC curve analysis for diagnostic showed AUC values of 0.976 for CXCL10, 0.777 for PDCD1, 0.837 for TIGIT, 0.946 for FOXP3, 0.528 for IL17A, and 0.626 for CD274, highlighting their potential clinical value (Figure 6D). These findings implied that CXCL10, PDCD1, TIGIT, and FOXP3 may function as relevant biomarkers for predicting patient survival. This model also demonstrated good calibration performance. Future studies should focus on improving the reliability and clinical utility of these biomarkers, particularly by exploring their combined effects to improve prognostic tools for ovarian cancer patients.

Expression and Functional Study of CXCL10 in Ovarian Cancer Cells

This study compared CXCL10 expression in ovarian cancer cell lines: OVCAR3, SKOV3, A2780, and ES2. Among these, CXCL10 levels were significantly higher in the A2780 cells ($p < 0.01$) (Figure 7A). Fluorescence microscopy images confirmed successful transfection and normal morphology after CXCL10 overexpression or knockout in SKOV3 and A2780 cells (Figure 7B). Western blot analysis supported these

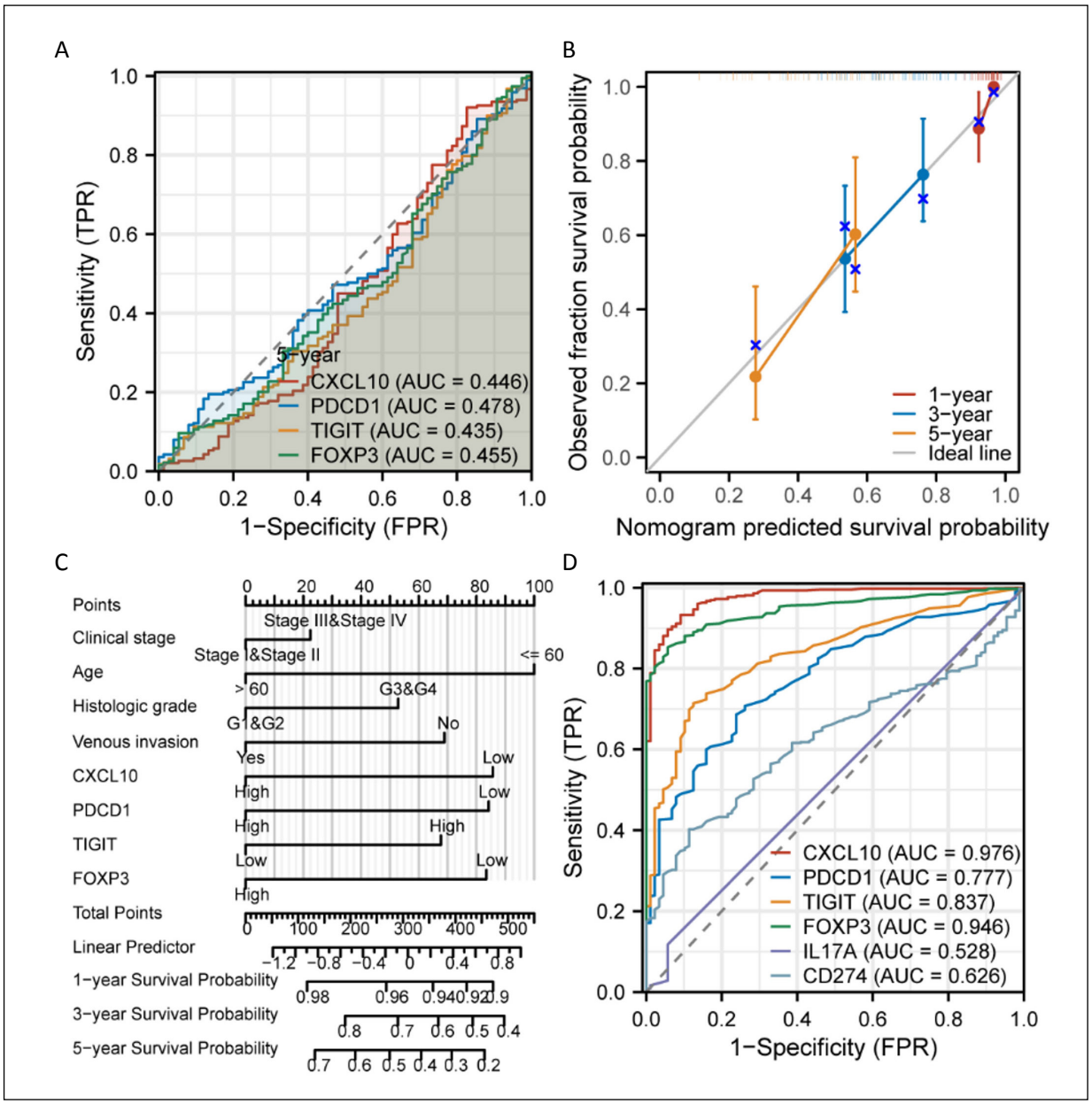

Figure 6. Prognostic performance of C-X-C motif chemokine ligand 10 (CXCL10), programmed cell death 1 (PDCD1), T cell immunoreceptor with Ig and ITIM domains (TIGIT), and forkhead box P3 (FOXP3). *A*, Time-dependent receiver operating characteristic (ROC) curve show area under the curve (AUC) values of 0.446, 0.478, 0.435, and 0.455 for these biomarkers in five-year survival prediction. *B*, The nomogram calibration curves compare predicted probabilities with actual survival outcomes, demonstrating satisfactory calibration for 1-, 3-, and 5-year survival. *C*, The nomogram integrates clinical features and biomarker scores, calculating the weighted impact of each to predict patient survival probabilities. *D*, The ROC curves for CXCL10, PDCD1, TIGIT, FOXP3, interleukin-17A (IL17A), and programmed death-ligand 1 (CD274 or PD-L1) show AUC values of 0.976, 0.777, 0.837, 0.946, 0.528, and 0.626, respectively, suggesting their potential utility in clinical practice.

findings, using β-actin as the loading control (Figure 7C). Grayscale analysis demonstrated that CXCL10 protein levels were significantly increased in the SKOV3-CXCL10 overexpression group compared to the control group (Figure 7D). These results confirmed the regulatory role of CXCL10 in ovarian cancer, with A2780 showing the highest expression and SKOV3 lower expression. Lentivirus-mediated CXCL10 overexpression and knockout experiments established valuable cell models for further functional studies. SKCM samples with high CXCL10 levels had significantly higher therapeutic scores than those with low levels ($p < 0.001$) (Figure 7E). A similar trend was observed in TCGA_OV ovarian cancer specimens, where high CXCL10 expression correlated with superior therapeutic scores ($p < 0.001$) (Figure 7F).

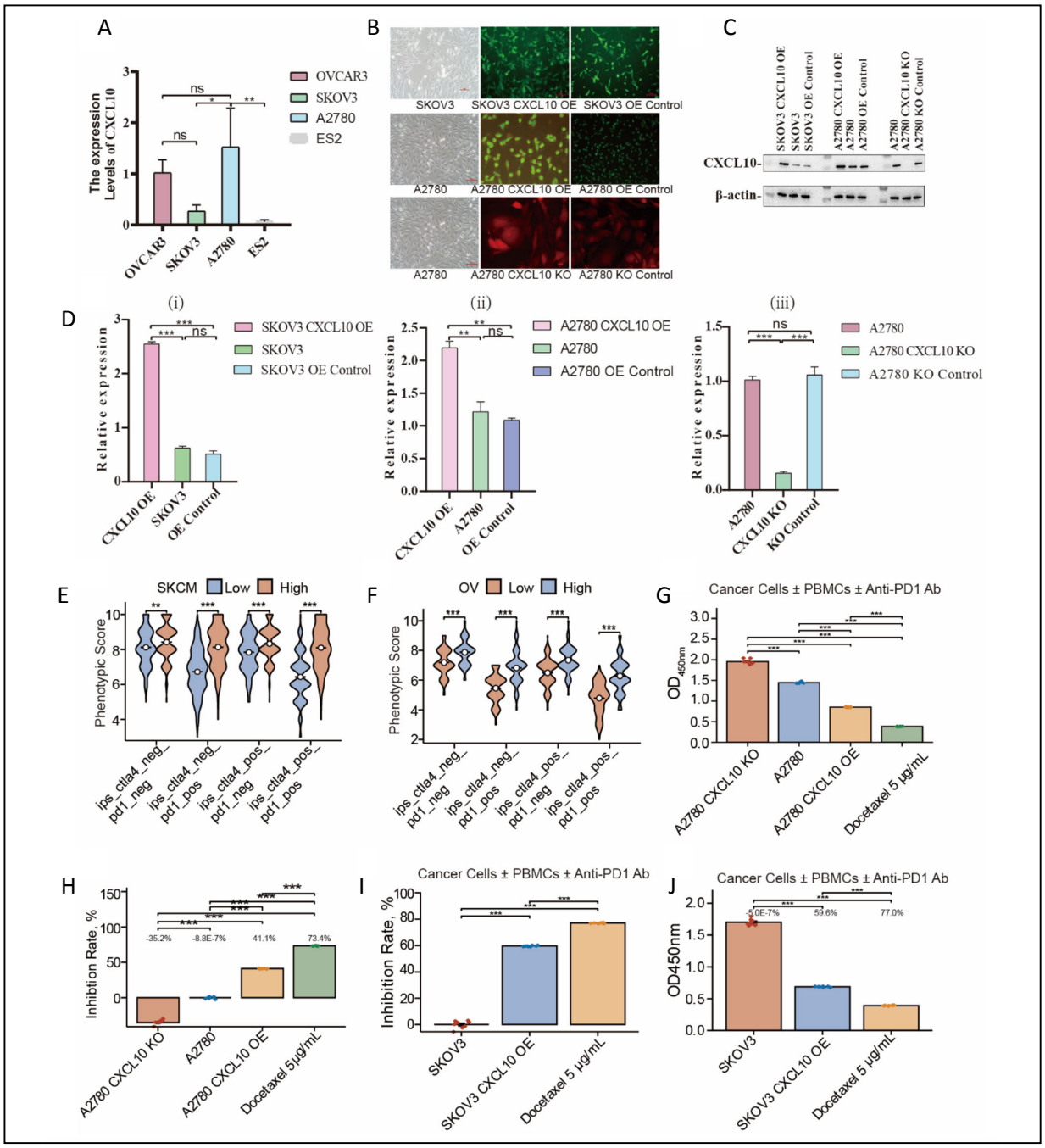

Figure 7. Analysis of treatment scores and cell proliferation effects of C-X-C motif chemokine ligand 10 (CXCL10) in ovarian cancer. *A*, CXCL10 expression varies among cell lines. A2780 shows significantly higher levels than other cell lines ($p < 0.01$). *B*, Fluorescence microscopy reveals successful transfection in SKOV3 and A2780 cells following CXCL10 overexpression or knockout. *C*, Western blot confirms CXCL10 protein levels using beta-actin (β-actin) as the loading control. *D*, Grayscale analysis shows that SKOV3-CXCL10 overexpression (SKOV3-CXCL10 OE) cells have significantly elevated CXCL10 levels, while A2780-CXCL10 knockout (A2780-CXCL10 KO) cells show decreased levels compared to controls ($p < 0.01$). *E*, Skin cutaneous melanoma (SKCM) samples with high CXCL10 expression demonstrates higher treatment scores compared with low CXCL10 groups. *F*, Comparison of treatment scores in The Cancer Genome Atlas–ovarian cancer (TCGA-OV) samples reveal the impact of varying CXCL10 expression levels. *G*, In A2780 cells, anti-programmed cell death protein 1 (PD-1) antibody treatment significantly alters proliferation between CXCL10 overexpressing and knockout cell lines, with additional variation observed under peripheral blood mononuclear cells (PBMCs) co-culture conditions. *H*, The inhibition rate of proliferation was significantly higher in the CXCL10 overexpressing group compared with other A2780-derived cells. *I*, Anti-PD-1 antibody treatment results in distinct proliferation outcomes in SKOV3 CXCL10 overexpressing cell lines and PBMCs co-cultured cells. *J*, The CXCL10 overexpressing group in SKOV3-derived cells exhibits a significantly greater proliferation inhibition compared with SKOV3 control and knockout groups. Statistical significance is indicated as follows: *** $p < 0.001$; ** $p < 0.01$; * $p < 0.05$.

Elevated CXCL10 expression improved clinical outcomes in PDCD1-positive patients, suggesting better treatment response. Proliferation assays on A2780 cells treated with anti-PD-1 antibody revealed decreased proliferation rates in CXCL10-overexpressing cells (Figure 7G). The CXCL10 overexpression cohort exhibited a significantly higher inhibition rate compared to other groups ($p < 0.001$) (Figure 7H). Similar trends were observed in the SKOV3 cell line (Figure 7I), with CXCL10 overexpression leading to reduced proliferation. There was a statistically significant difference in inhibition rates between the CXCL10 overexpression cohort and the control cohort ($p < 0.01$) (Figure 7J). Overall, these findings highlighted a strong link between elevated CXCL10 expression and improved therapeutic efficacy and reduced cellular proliferation. These results offered novel perspectives for optimizing immunotherapeutic strategies.

DISCUSSION

Ovarian cancer (OV) ranks among the most lethal malignancies of the female reproductive system, and its global incidence is rising annually[43,44]. The global incidence rate is 6.8 per 100,000, with most cases diagnosed at advanced stages. Therefore, early identification and intervention are crucial for improving patient survival outcomes. Early diagnosis is challenging due to ambiguous symptoms and the lack of effective early detection methods, posing significant difficulties in clinical management. Therefore, it is essential to investigate novel biomarkers that facilitate early diagnosis and refine therapeutic approaches.

This investigation systematically elucidated the pivotal function of the chemokine CXCL10 within the tumor microenvironment by conducting differential gene expression analyses of ovarian cancer specimens obtained from GTEx and TCGA. Volcano plots and heatmaps showed significant upregulation of CXCL10 and other chemokines in tumor tissues, with the elevation of CXCL10 being significantly correlated with the infiltration of T cells and macrophages ($p < 0.001$). Pathway enrichment analysis revealed activation of the interferon-gamma signaling pathway (FDR < 0.01), the antigen presentation pathway (FDR < 0.05), and the T cell activation pathway, highlighting CXCL10's central role in orchestrating antitumor immune responses. These results offer novel perspectives on the mechanisms underlying immune evasion in ovarian cancer and establish a foundational basis for prospective immunotherapeutic interventions.

Immunotherapy has emerged as a transformative therapeutic modality in oncology, but its application in ovarian cancer faces substantial challenges. Immune checkpoint inhibitors, particularly PD-1/PD-L1 inhibitors, show objective response rates below 15% as monotherapy in ovarian cancer. This is lower than their 20-40% response rates observed in other solid tumors[45,46]. The limited efficacy of immune checkpoint inhibitors mainly results from ovarian cancer's unique immunosuppressive microenvironment. It is characterized by infiltration of regulatory T cells and tumor-associated macrophages, as well as a relatively low tumor mutational burden that restricts neoantigen generation[47,48]. Additionally, ascites creates an immunosuppressive microenvironment that inhibits immune effector cell function by releasing immunosuppressive cytokines and imposing metabolic constraints[49]. Our findings demonstrate that CXCL10 and immune checkpoints, including PDCD1 (PD-1), TIGIT, and FOXP3, represent promising targets for synergistic therapeutic strategies. Furthermore, survival analysis reveals that patients with higher expression of CXCL10 and these immune checkpoints survive significantly longer than those with lower levels (HR < 1), supporting their role as favorable prognostic markers. Furthermore, evidence suggests that BRCA1/2 deficiency enhances CXCL10 levels and CD8 T cell infiltration in ovarian cancer, with activation of STING pathway leading to pronounced CXCL10 expression in BRCA1-deficient tumors[50,51].

Our investigation identifies CXCL10 as a crucial modulator of the ovarian cancer immune microenvironment. It also highlights important implications for precision oncology by demonstrating correlations with CD8 T cell infiltration and immune checkpoint activation. However, this study has limitations, including its retrospective design and absence of BRCA1/2 mutation analysis. Future research should focus on the cGAS-STING-CXCL10 axis in BRCA-deficient tumors to define its contribution to antitumor immune activation. CXCL10 together with BRCA1/2 should be prospectively validated as composite biomarkers, assessing their joint performance for predicting immunotherapy benefit and guiding patient stratification. Therapeutic development should evaluate CXCL10-centered strategies, including rational combinations with PD-1 blockade to potentiate T-cell–mediated control and the design of CXCL10-directed bispecific antibodies to enhance immune recruitment. Standardization of clinical detection protocols, coupled with rigorous validation in well-designed prospective trials and mechanistic studies, will be essential to enable clinical implementation and advance personalized immunotherapy for ovarian cancer.

Authors' Contributions:

Lin Deng: Conceptualization, Methodology, Software, Validation, Formal Analysis, Investigation, Resources, Data Curation, Writing - Original Draft, Writing - Review & Editing, Visualization. Wenhong Lin: Methodology, Software, Validation, Formal Analysis, Investigation, Resources, Data Curation, Writing - Review & Editing. Fumei Jian: Methodology, Software, Validation, Formal Analysis, Investigation, Resources, Data Curation, Writing - Review & Editing. Dunsong Fan: Methodology, Software, Validation, Formal Analysis, Investigation, Resources, Data Curation, Writing - Review & Editing. Jianming Lan: Resources, Data Curation, Writing - Review & Editing, Supervision. Dongxia Liao: Resources, Data Curation, Writing - Review & Editing, Supervision. Peiyuan Luo: Conceptualization, Methodology, Supervision, Project Administration, Funding Acquisition, Writing - Review & Editing. The final approval of the version to be published is approved by all authors; and that all authors agree to be accountable for all aspects of the work.

Acknowledgments:

We acknowledge the importance of open science and data sharing in advancing cancer research. All raw data and analysis protocols have been made publicly available to support reproducible research and enable independent verification of our findings. We are grateful to the research community for maintaining open-access databases that facilitate scientific discovery and collaboration.

Conflict of Interest :

The authors declare no conflicts of interest regarding the publication of this paper.

Funding:

This work was supported by the Startup Fund for Scientific Research at Fujian Medical University (Grant Number: 2023QH1362). The funders had no role in the study design, data collection and analysis, decision to publish, or preparation of the manuscript.

Data Availability Statement:

The data used in this study are available upon request from the corresponding author. The study findings are supported by data from The Cancer Genome Atlas (TCGA, https://portal.gdc.cancer.gov/), specifically ovarian cancer datasets (reference number available upon request). Relevant GEO datasets (https://www.ncbi.nlm.nih.gov/geo/) include GSE10971, GSE14407, and GSE18520. If applicable, data were also sourced from the Cancer Imaging Archive (TCIA, specific reference available upon request).
The raw data supporting the conclusions of this article are openly available in the Zenodo repository at https://zenodo.org/records/17207352 (DOI: 10.5281/zenodo.17207352).

Ethics Approval and Informed Consent:

The study did not involve animal experiments or human participants; therefore, the ethics approval and informed consent are not applicable.

REFERENCES

1. Barbieri F, Bajetto A, Florio T. Role of chemokine network in the development and progression of ovarian cancer: a potential novel pharmacological target. J Oncol 2010; 2010: 426956.
2. Torre LA, Trabert B, DeSantis CE, Miller KD, Samimi G, Runowicz CD, Gaudet MM, Jemal A, Siegel RL. Ovarian cancer statistics, 2018. CA Cancer J Clin 2018; 68: 284-296.
3. Sun G, Liu Y. Tertiary lymphoid structures in ovarian cancer. Front Immunol 2024; 15: 1465516.
4. MacFawn IP, Magnon G, Gorecki G, et al. The activity of tertiary lymphoid structures in high grade serous ovarian cancer is governed by site, stroma, and cellular interactions. Cancer Cell 2024; 42: 1864-1881 e5.
5. Chai C, Liang L, Mikkelsen NS, et al. Single-cell transcriptome analysis of epithelial, immune, and stromal signatures and interactions in human ovarian cancer. Commun Biol 2024; 7: 131.
6. Iyer S, Zhang S, Farkkila A, et al. Abstract B61: The genotype of serous carcinomas shapes the tumor microenvironment and modulates responses to targeted and immune checkpoint therapies. Clinical Cancer Research 2020; 26: B61.
7. Al Ashi SI, Thapa B, Flores M, Ahmed R, Rahim SEG, Amir M, Alomari M, Chadalavada P, Morrison SL, Bena JF, Hercbergs A, Lashin O, Daw H. Endocrine Toxicity and Outcomes in Patients With Metastatic Malignancies Treated With Immune Checkpoint Inhibitors. J Endocr Soc 2021; 5: bvab100.
8. Okoye IS, Houghton M, Tyrrell L, Barakat K, Elahi S. Coinhibitory Receptor Expression and Immune Checkpoint Blockade: Maintaining a Balance in CD8(+) T Cell Responses to Chronic Viral Infections and Cancer. Front Immunol 2017; 8: 1215.
9. Launonen IM, Niemiec I, Hincapié-Otero M, Erkan EP, Junquera A, Afenteva D, Falco MM, Liang Z, Salko M, Chamchougia F, Szabo A, Perez-Villatoro F, Li Y, Micoli G, Nagaraj A, Haltia UM, Kahelin E, Oikkonen J, Hynninen J, Virtanen A, Nirmal AJ, Vallius T, Hautaniemi S, Sorger PK, Vähärautio A, Färkkilä A. Chemotherapy induces myeloid-driven spatially confined T cell exhaustion in ovarian cancer. Cancer Cell 2024; 42: 2045-2063 e10.

10. He S, Ma L, Cheng G, et al. Abstract B105: The impact of cholesterol and its metabolites on ovarian tumor microenvironment and cancer progression. 2020; 8 (3_Supplement): B105.
11. Dong M, Lu L, Xu H, Ruan Z. DC-derived CXCL10 promotes CTL activation to suppress ovarian cancer. Transl Res 2024; 272: 126-139.
12. Xu Z, Zhang X, Lau J, Yu J. C-X-C motif chemokine 10 in non-alcoholic steatohepatitis: role as a pro-inflammatory factor and clinical implication. Expert Rev Mol Med 2016; 18: e16.
13. Zou W. Abstract IA18: Metabolic impact on cancer immunity. 2020; 26 (13_Supplement): IA18.
14. Yen JH, Chang CC, Hsu HJ, Yang CH, Mani H, Liou JW. C-X-C motif chemokine ligand 12-C-X-C chemokine receptor type 4 signaling axis in cancer and the development of chemotherapeutic molecules. Tzu Chi Med J 2024; 36: 231-239.
15. Qin R, Ren W, Ya G, Wang B, He J, Ren S, Jiang L, Zhao S. Role of chemokines in the crosstalk between tumor and tumor-associated macrophages. Clin Exp Med 2023; 23: 1359-1373.
16. Rainczuk A, Rao J, Gathercole J, Stephens AN. The emerging role of CXC chemokines in epithelial ovarian cancer. Reproduction 2012; 144: 303-317.
17. Wang Z, Ou Q, Liu Y, Liu Y, Zhu Q, Feng J, Han F, Gao L. Adipocyte-derived CXCL10 in obesity promotes the migration and invasion of ovarian cancer cells. J Ovarian Res 2024; 17: 245.
18. Consortium GT. The Genotype-Tissue Expression (GTEx) project. Nat Genet 2013; 45: 580-585.
19. Cancer Genome Atlas Research Network; Weinstein JN, Collisson EA, Mills GB, Shaw KR, Ozenberger BA, Ellrott K, Shmulevich I, Sander C, Stuart JM. The Cancer Genome Atlas Pan-Cancer analysis project. Nat Genet 2013; 45: 1113-1120.
20. Love MI, Huber W, Anders S. Moderated estimation of fold change and dispersion for RNA-seq data with DESeq2. Genome Biol 2014; 15: 550.
21. Soneson C, Delorenzi M. A comparison of methods for differential expression analysis of RNA-seq data. BMC Bioinformatics 2013; 14: 91.
22. Ritchie ME, Phipson B, Wu D, Hu Y, Law CW, Shi W, Smyth GK. limma powers differential expression analyses for RNA-sequencing and microarray studies. Nucleic Acids Research 2015; 43: e47-e47.
23. Subramanian A, Tamayo P, Mootha VK, Mukherjee S, Ebert BL, Gillette MA, Paulovich A, Pomeroy SL, Golub TR, Lander ES, Mesirov JP. Gene set enrichment analysis: a knowledge-based approach for interpreting genome-wide expression profiles. Proc Natl Acad Sci U S A 2005; 102: 15545-15550.
24. Li J, Yue H, Yu H, Lu X, Xue X. Patients with low nicotinamide N-methyltransferase expression benefit significantly from bevacizumab treatment in ovarian cancer. BMC Cancer 2021; 21: 67.
25. Song C, Kim KB, Lee JH, Kim S. Bioinformatic Analysis for Influential Core Gene Identification and Prognostic Significance in Advanced Serous Ovarian Carcinoma. Medicina (Kaunas) 2021; 57: 933.
26. Li Y, Li L. Prognostic values and prospective pathway signaling of MicroRNA-182 in ovarian cancer: a study based on gene expression omnibus (GEO) and bioinformatics analysis. Journal of Ovarian Research 2019; 12: 106.
27. Gov E, Arga KY. Differential co-expression analysis reveals a novel prognostic gene module in ovarian cancer. Sci Rep 2017; 7: 4996.
28. Gustavsson EK, Zhang D, Reynolds RH, Garcia-Ruiz S, Ryten M. ggtranscript: an R package for the visualization and interpretation of transcript isoforms using ggplot2. Bioinformatics 2022; 38: 3844-3846.
29. Gao CH, Yu G, Cai P. ggVennDiagram: An Intuitive, Easy-to-Use, and Highly Customizable R Package to Generate Venn Diagram. Front Genet 2021; 12: 706907.
30. Szklarczyk D, Gable AL, Nastou KC, Lyon D, Kirsch R, Pyysalo S, Doncheva NT, Legeay M, Fang T, Bork P, Jensen LJ, von Mering C. The STRING database in 2021: customizable protein–protein networks, and functional characterization of user-uploaded gene/measurement sets. Nucleic Acids Research 2021; 49: D605-D612.
31. Yu G, Wang LG, Han Y, He QY. clusterProfiler: an R package for comparing biological themes among gene clusters. Omics 2012; 16: 284-287.
32. Song Y, Zhang J, Zhang L, Zhang S, Shen C. PDP1 Promotes Cell Malignant Behavior and Is Associated with Worse Clinical Features in Ovarian Cancer Patients: Evidence from Bioinformatics and In Vitro Level. Comput Math Methods Med 2022; 2022: 7397250.
33. Liu J, Zhang D, Cao Y, Zhang H, Li J, Xu J, Yu L, Ye S, Yang L. Screening of crosstalk and pyroptosis-related genes linking periodontitis and osteoporosis based on bioinformatics and machine learning. Front Immunol 2022; 13: 955441.
34. Chen B, Khodadoust MS, Liu CL, Newman AM, Alizadeh AA. Profiling Tumor Infiltrating Immune Cells with CIBERSORT. Methods Mol Biol 2018; 1711: 243-259.
35. Liu J, Lichtenberg T, Hoadley KA, Poisson LM, Lazar AJ, Cherniack AD, Kovatich AJ, Benz CC, Levine DA, Lee AV, Omberg L, Wolf DM, Shriver CD, Thorsson V; Cancer Genome Atlas Research Network; Hu H. An Integrated TCGA Pan-Cancer Clinical Data Resource to Drive High-Quality Survival Outcome Analytics. Cell 2018; 173: 400-416.e11.
36. Wu X, Rong L, Tang R, Li Q, Wang F, Deng X, Miao L. Unveiling the role of CXCL10 in pancreatic cancer progression: A novel prognostic indicator. Open Med (Wars) 2025; 20: 20241117.
37. Vivian J, Rao AA, Nothaft FA, Ketchum C, Armstrong J, Novak A, Pfeil J, Narkizian J, Deran AD, Musselman-Brown A, Schmidt H, Amstutz P, Craft B, Goldman M, Rosenbloom K, Cline M, O'Connor B, Hanna M, Birger C, Kent WJ, Patterson DA, Joseph AD, Zhu J, Zaranek S, Getz G, Haussler D, Paten B. Toil enables reproducible, open source, big biomedical data analyses. Nat Biotechnol 2017; 35: 314-316.
38. Li J, Guan Y, Zhu R, Wang Y, Zhu H, Wang X. Identification of metabolic genes for the prediction of prognosis and tumor microenvironment infiltration in early-stage non-small cell lung cancer. Open Life Sci 2022; 17: 881-892.
39. Zhou L, Li SH, Wu Y, Xin L. Establishment of a prognostic model of four genes in gastric cancer based on multiple data sets. Cancer Med 2021; 10: 3309-3322.
40. Shen KY, Chen BY, Gao WC. Single-Cell RNA Sequencing Reveals the Role of Epithelial Cell Marker Genes in Predicting the Prognosis of Colorectal Cancer Patients. Dis Markers 2022; 2022: 8347125.
41. Luo Z, Wang Y, Bi X, Ismtula D, Wang H, Guo C. Cytokine-induced apoptosis inhibitor 1: a comprehensive analysis of potential diagnostic, prognosis, and immune biomarkers in invasive breast cancer. Transl Cancer Res 2023; 12: 1765-1786.

42. Zhang P, Chen D, Cui H, Luo Q. High Expression of CHST11 Correlates with Poor Prognosis and Tumor Immune Infiltration of Pancreatic Cancer. Clin Lab 2022; 68: 211-239.
43. Zhang J, Chen Y, Chen X, Zhang W, Zhao L, Weng L, Tian H, Wu Z, Tan X, Ge X, Wang P, Fang L. Deubiquitinase USP35 restrains STING-mediated interferon signaling in ovarian cancer. Cell Death Differ 2021; 28: 139-155.
44. Ouyang Q, Liu Y, Tan J, Li J, Yang D, Zeng F, Huang W, Kong Y, Liu Z, Zhou H, Liu Y. Loss of ZNF587B and SULF1 contributed to cisplatin resistance in ovarian cancer cell lines based on Genome-scale CRISPR/Cas9 screening. Am J Cancer Res 2019; 9: 988-998.
45. Matulonis UA, Shapira-Frommer R, Santin AD, Lisyanskaya AS, Pignata S, Vergote I, Raspagliesi F, Sonke GS, Birrer M, Provencher DM, Sehouli J, Colombo N, González-Martín A, Oaknin A, Ottevanger PB, Rudaitis V, Katchar K, Wu H, Keefe S, Ruman J, Ledermann JA. Antitumor activity and safety of pembrolizumab in patients with advanced recurrent ovarian cancer: results from the phase II KEYNOTE-100 study. Ann Oncol 2019; 30: 1080-1087.
46. Hamanishi J, Mandai M, Ikeda T, Minami M, Kawaguchi A, Murayama T, Kanai M, Mori Y, Matsumoto S, Chikuma S, Matsumura N, Abiko K, Baba T, Yamaguchi K, Ueda A, Hosoe Y, Morita S, Yokode M, Shimizu A, Honjo T, Konishi I. Safety and Antitumor Activity of Anti-PD-1 Antibody, Nivolumab, in Patients With Platinum-Resistant Ovarian Cancer. J Clin Oncol 2015; 33: 4015-4022.
47. Zhang L, Conejo-Garcia JR, Katsaros D, Gimotty PA, Massobrio M, Regnani G, Makrigiannakis A, Gray H, Schlienger K, Liebman MN, Rubin SC, Coukos G. Intratumoral T cells, recurrence, and survival in epithelial ovarian cancer. N Engl J Med 2003; 348: 203-213.
48. Chalmers ZR, Connelly CF, Fabrizio D, Gay L, Ali SM, Ennis R, Schrock A, Campbell B, Shlien A, Chmielecki J, Huang F, He Y, Sun J, Tabori U, Kennedy M, Lieber DS, Roels S, White J, Otto GA, Ross JS, Garraway L, Miller VA, Stephens PJ, Frampton GM. Analysis of 100,000 human cancer genomes reveals the landscape of tumor mutational burden. Genome Med 2017; 9: 34-47.
49. Bodnar RJ, Yates CC, Wells A. IP-10 blocks vascular endothelial growth factor-induced endothelial cell motility and tube formation via inhibition of calpain. Circ Res 2006; 98: 617-625.
50. Vázquez-García I, Uhlitz F, Ceglia N, Lim JLP, Wu M, Mohibullah N, Niyazov J, Ruiz AEB, Boehm KM, Bojilova V, Fong CJ, Funnell T, Grewal D, Havasov E, Leung S, Pasha A, Patel DM, Pourmaleki M, Rusk N, Shi H, Vanguri R, Williams MJ, Zhang AW, Broach V, Chi DS, Da Cruz Paula A, Gardner GJ, Kim SH, Lennon M, Long Roche K, Sonoda Y, Zivanovic O, Kundra R, Viale A, Derakhshan FN, Geneslaw L, Issa Bhaloo S, Maroldi A, Nunez R, Pareja F, Stylianou A, Vahdatinia M, Bykov Y, Grisham RN, Liu YL, Lakhman Y, Nikolovski I, Kelly D, Gao J, Schietinger A, Hollmann TJ, Bakhoum SF, Soslow RA, Ellenson LH, Abu-Rustum NR, Aghajanian C, Friedman CF, McPherson A, Weigelt B, Zamarin D, Shah SP. Ovarian cancer mutational processes drive site-specific immune evasion. Nature 2022; 612: 778-786.
51. Bruand M, Barras D, Mina M, Ghisoni E, Morotti M, Lanitis E, Fahr N, Desbuisson M, Grimm A, Zhang H, Chong C, Dagher J, Chee S, Tsianou T, Dorier J, Stevenson BJ, Iseli C, Ronet C, Bobisse S, Genolet R, Walton J, Bassani-Sternberg M, Kandalaft LE, Ren B, McNeish I, Swisher E, Harari A, Delorenzi M, Ciriello G, Irving M, Rusakiewicz S, Foukas PG, Martinon F, Dangaj Laniti D, Coukos G. Cell-autonomous inflammation of BRCA1-deficient ovarian cancers drives both tumor-intrinsic immunoreactivity and immune resistance via STING. Cell Rep 2021; 36: 109412.